ACS APPLIED MATERIALS & INTERFACES

LETTER

www.acsami.org

Ferroelectric Behavior in Bismuth Ferrite Thin Films of Different Thickness

Jiagang Wu,[†,*] John Wang,[‡] Dingquan Xiao,[†] and Jianguo Zhu[†]

[†]Department of Materials Science, Sichuan University, Chengdu 610064, P. R. China

[‡]Department of Materials Science and Engineering, National University of Singapore, Singapore 117574, Singapore

ABSTRACT: The ferroelectric behavior of $BiFeO_3$ thin films is modified by changing the film thicknesses, where the $BiFeO_3$ thin films with different thicknesses were grown on $SrRuO_3/Pt/TiO_2/SiO_2/Si(100)$ substrates by radio frequency sputtering. The mixture of (110) and (111) orientations is induced for all $BiFeO_3$ thin films regardless of their thicknesses, together with the columnar structure and the dense microstructure. Their dielectric behavior is almost independent of the film thickness where all thin films have a low dielectric loss. A giant remanent polarization of $2P_r \approx 156.6-188.8\ \mu C/cm^2$ is induced for the $BiFeO_3$ thin films in the thickness range of 190−600 nm. As a result, it is an effective way to improve the ferroelectric behavior of the $BiFeO_3$ thin film by tailoring the film thickness.

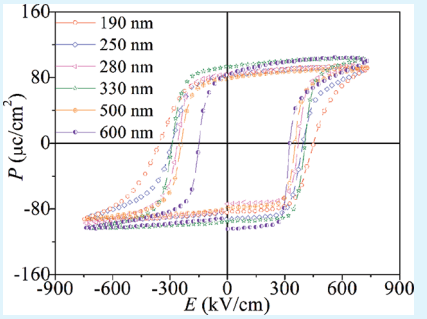

KEYWORDS: bismuth ferrite, thickness dependence, ferroelectric properties

1. INTRODUCTION

Considerable attention has been given to multiferroic ($BiMnO_3$, $TbMnO_3$, and $BiFeO_3$) materials because of the coexistence of ferroelectricity, (anti)ferromagnetism, and ferroelasticity.[1−6] Recently, the $BiFeO_3$ (BFO) material has been extensively studied from the viewpoint of device applications,[5−14] because of the Neel temperature ($T_N \approx 370$ °C), a high Curie temperature ($T_c \approx 850$ °C), and a giant polarization value confirmed by the theories[15] and the experiments.[16,17] According to the theoretical predication, an unusual spontaneous polarization (up to ∼100 $\mu C/cm^2$) has been predicted for the BFO material with (111) orientation.[15,16] A larger polarization has also been demonstrated for the epitaxial BFO thin films grown on $SrRuO_3/SrTiO_3$ substrates by pulse laser deposition,[6,16] but it is not integrated with other silicon devices because of the introduction of an expensive $SrTiO_3$ substrate. Moreover, a polycrystalline BFO thin film with a tetragonal structure is of a giant polarization value of $P_r \approx 150\ \mu C/cm^2$ when prepared on the $Pt/TiO_2/SiO_2/Si(100)$ substrate by pulsed laser deposition, but the measurement temperature is below room temperature (90 K).[13] Therefore, the expensive $SrTiO_3$ substrate and the low-temperature measurement technique hinder the practical applications considered for the bismuth ferrite thin films.

Some attempts have been conducted to improve the electrical properties of bismuth ferrite thin films, such as the employment of the film thickness effects,[18−22] ion substitution,[14] buffer layer,[23] and orientation.[16,17] There have been some works about the thickness dependence of electrical properties in BFO thin films by tailoring the film thicknesses, as listed in Table 1.[6,18−22] A high remanent polarization is often demonstrated for the BFO thin film with an optimum film thickness when grown on $SrRuO_3/SrTiO_3$ substrates.[6,18,19] However, BFO thin films grown in oxides buffer layer/silicon substrates exhibit a poorer ferroelectric behavior,[20,21] or the ferroelectric properties can be only measured at a low temperature.[22] It is highly desirable to prepare the BFO thin films on a silicon substrate to enable the integration with other Si devices, and the trend of miniaturization of devices requires the reduction in the thickness of thin films. However, the direct growth of BFO thin films on Pt-coated silicon substrate often results in the formation of a dead layer at the interface and the generation of secondary phases,[23] but BFO thin films can be well grown on Pt-coated silicon via several oxide buffer layers including $SrRuO_3$,[17] $BaPbO_3$,[20] $LaNiO_3$,[24] and (La, Sr)MnO_3.[25]

In the present work, we modify the thickness of BFO thin films grown on oxide buffer layer $SrRuO_3/Pt/TiO_2/SiO_2/Si(100)$ substrates by radio frequency (rf) sputtering. The thickness dependence of ferroelectric behavior in BFO thin films is studied. A giant polarization is demonstrated for the BFO thin films grown on silicon substrates by modifying the film thickness.

2. EXPERIMENTAL PROCEDURE

A ceramic target of $Bi_{1.15}FeO_3$ was sintered by the mixed oxides of Bi_2O_3 and Fe_2O_3. These powders were mixed by the ball milling for 24 h, and then the powder was calcined at ∼720 °C for 6 h after drying. The calcined powder mixture was pressed into a two-inch pellet and then the pellet was sintered at ∼820 °C for 2 h. The $SrRuO_3$ buffer layer with a thickness of ∼90 nm is first grown on $Pt/TiO_2/SiO_2/Si(100)$ substrates by rf sputtering, and then the BFO thin films with the thickness range of 100−600 nm were deposited on $SrRuO_3/Pt/TiO_2/SiO_2/Si(100)$ substrates by rf sputtering at the substrate temperatures of ∼570 °C. They were both deposited under a rf power of 120 W, and at a base pressure of 3.0×10^{-6} Torr and a deposition pressure of 10 mTorr with Ar and O_2 at a ratio of 4:1. Circular Pt electrodes of 0.20 mm in diameter were prepared on the thin films by rf sputtering through a shadow mask for measuring electrical properties of thin films.

Received: June 21, 2011
Accepted: August 23, 2011
Published: August 23, 2011

Table 1. Thickness-Dependent Electrical Properties for the Bismuth Ferrite Thin Films

composition	substrate	thickness (nm)	preparation method	orientation	$2P_r$ ($\mu C/cm^2$)	ref
BFO	$SrRuO_3/SrTiO_3(100)$		PLD	(100)	110	6
BFO	$SrRuO_3/SrTiO_3(001)$	450	RF	(001)	170	18
Mn-BFO	$SrRuO_3/SrTiO_3(001)$	70	PLD	(001)	130	19
BFO	$BaPbO_3/Pt/Ti/SiO_x/Si$	230	RF	polycrystal	85.6	20
BFO	$LaNiO_3/Pt/Ti/SiO_2/Si$	115	sol−gel	polycrystal	28.6	21
BFO	$Pt/Ti/SiO_2/Si$	400	CSD	polycrystal	180 at 80 K	22
BFO	$SrRuO_3/Pt/Ti/SiO_2/Si$	330	RF	(110)/(111)	188.8 ± 0.2	in this work

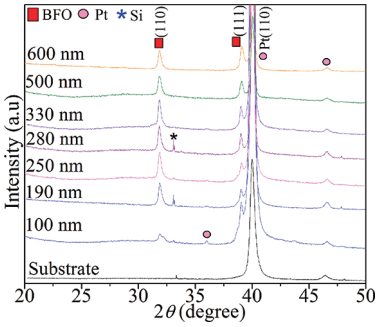

Figure 1. XRD patterns of $BiFeO_3$ thin films with different thicknesses.

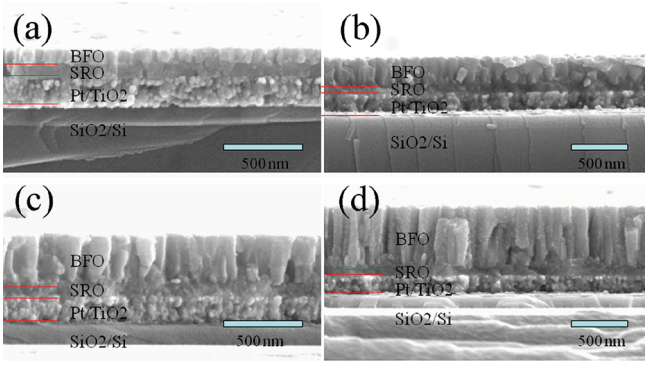

Figure 2. Cross-section of $BiFeO_3$ thin films with different thicknesses of (a) 100, (b) 250 nm, (c) 330 nm, and (d) 600 nm.

Crystal structures of thin films were measured by X-ray diffraction (XRD) analysis using DX1000 (Dandong, China). Scanning electron microscopy (SEM) (Philips, XL30) was employed to study the cross section of thin films. An impedance analyzer (Solartron Gain phase Analyzer) was employed to measure their dielectric properties, and the ferroelectric behavior is measured by RT2000 Tester (USA).

3. RESULTS AND DISCUSSION

Figure 1 shows the XRD patterns for the BFO thin films with different thicknesses. All thin films possess a pure phase, and no secondary phases are detected. Moreover, the mixture of (110) and (111) orientations is demonstrated for all thin films, as shown by the strong and sharp (110) and (111) peaks, independent of the film thicknesses.

Figure 2 shows the SEM cross sectional images for the BFO thin films with different thicknesses. All thin films have a columnar structure, and the interface among thin film, SRO buffer layer, and Pt electrode is well-established, indicating that

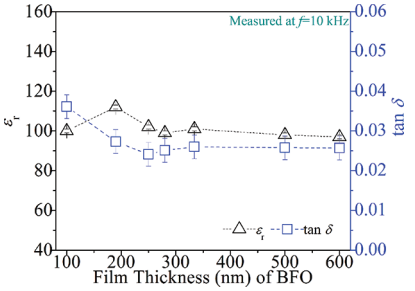

Figure 3. Dielectric behavior of $BiFeO_3$ thin films with different thicknesses, measured at 10 kHz.

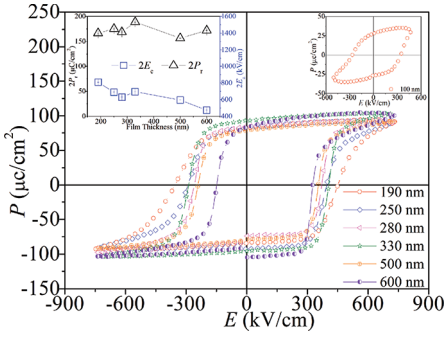

Figure 4. $P-E$ loops of $BiFeO_3$ thin films with different thicknesses, where the inserts are $2P_r$ and $2E_c$ values as a function of applied electric fields and the $P-E$ loop for the BFO thin film with a 100 nm thickness.

the BFO layer is well-sputtered on the bottom of the SRO buffer layer. The substantial diffusion between two different phases is not observed. The typical columnar structure in this work confirms that the BFO thin film is well-crystallized.

Figure 3 plots the dielectric constant (ε_r) and the dielectric loss (tan δ) of BFO thin films as a function of the film thicknesses, measured at the frequency of 10 kHz and room temperature. The dielectric behavior slightly changes for all BFO thin films in the range of the film thicknesses investigated, confirming that the dielectric behavior is almost independent of the thicknesses of BFO thin films in the present work. The dead layer forming in the interface between the film and bottom electrode is often responsible for the decrease in ε_r. In the present work, the interface between BFO and SRO is well established in Figure 2, resulting in a constant of ε_r value. Moreover, the dense microstructure in Figure 2 contributes to the low tan δ value in these BFO thin films.

Figure 4 plots the $P-E$ loops for the BFO thin films with different thicknesses, measured at f = 1 kHz and room

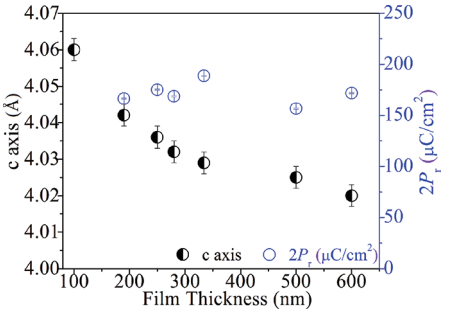

Figure 5. Summary of the thickness dependence of out-of-plane lattice parameter and polarization.

temperature. All BFO thin films exhibit similar ferroelectric behavior except for the $P-E$ loop of the BFO thin film with a ~100 nm thickness, where a low remanent polarization is induced because of a higher leakage current density of too thin thickness (100 nm) caused by a tunneling effect, as shown in the insert of Figure 4. The insert in Figure 4 shows the $2P_r$ and $2E_c$ values as a function of applied electric fields for the BFO thin films with the thicknesses of 190−600 nm. The $2P_r$ values almost keep unchanged for all thin films with the thicknesses of 190−600 nm. Moreover, the thicker BFO thin films, the smaller $2E_c$ values. The $2E_c$ value is ~808 kV/cm for the BFO thin film with 190 nm thickness, and then the $2E_c$ value decreases with an increase in the film thickness. This phenomenon is attributed to the change in the strain relaxation with the film thickness.[19,26,27] In the present work, the $2P_r$ value is much larger than those of BFO thin films reported by other authors.[6,10,12,14,18−22] It has been reported that the polarization of BFO thin films is almost independent of the strain, as confirmed by the first-principle calculation and the experimental result.[27,28] In this work, the polarization of BFO thin films with 190−600 nm thickness is weakly dependent on the strain, as shown in Figure 5, where the ferroelectric behavior of BFO thin films with 100 nm thickness cannot be measured at room temperature due to the electrical conductivity. The improvement in ferroelectric properties of BFO thin films can be attributed to the mixture of (111) and (110) orientations in this work, where the largest spontaneous polarization happens in the (111) direction for the BFO thin films because that the ions are displaced along [111] directions from their equilibrium positions.[29,30] Therefore, the mixture of (110) and (111) orientations largely contributes to the enhancement in ferroelectric properties of BFO thin films. The columnar structure and dense microstructure also partly contribute to the reduction in the leakage current density of BFO thin films, partly resulting in the improvement in its ferroelectric properties.

In summary, the effect of the thickness on the ferroelectric behavior of $BiFeO_3$ thin films, which were grown on $SrRuO_3$/Pt/TiO_2/SiO_2/Si(100) substrates by radio frequency sputtering, is investigated. The column structure and dense microstructure are demonstrated for all $BiFeO_3$ thin films with (110) and (111) orientations, together with a low dielectric loss. A giant remanent polarization has been induced for the $BiFeO_3$ thin film with an optimum thickness, confirming that the $BiFeO_3$ thin film is a promising candidate material for the memory device.

AUTHOR INFORMATION

Corresponding Author

*E-mail: msewujg@scu.edu.cn and wujiagang0208@163.com.

ACKNOWLEDGMENT

The authors gratefully acknowledge the supports of the National Natural Science Foundation of China (51102173), the Fundamental Research Funds for the Central Universities, the introduction of talent start funds of Sichuan University (2082204144033), and the National University of Singapore.

REFERENCES

(1) Lee, J. H.; Ke, X.; Misra, R.; Ihlefeld, J. F.; Xu, X. S.; Mei, Z. G.; Heeg, T.; Roeckerath, M.; Schubert, J.; Liu, Z. K.; Musfeldt, J. L.; Schiffer, P.; Schlom, D. G. *Appl. Phys. Lett.* **2010**, *96*, 262905.
(2) Hill, N. A.; Rabe, K. M. *Phys. Rev. B* **1999**, *59*, 8759–8769.
(3) Kitagawa, Y.; Hiraoka, Y.; Honda, T.; Ishikura, T.; Nakamura, H.; Kimura, T. *Nat. Mater.* **2010**, *9*, 797–802.
(4) Shuvaev, A. M.; Travkin, V. D.; Ivanov, V. Y.; Mukhin, A. A.; Pimenov, A. *Phys. Rev. Lett.* **2010**, *104*, 097202.
(5) Ramesh, R.; Spaldin, N. A. *Nat. Mater.* **2007**, *6*, 21–29.
(6) Wang, J.; Neaton, J. B.; Zheng, H.; Nagarajan, V.; Ogale, S. B.; Liu, B.; Viehland, D.; Vaithyanathan, V.; Schlom, D. G.; Waghmare, U. V.; Spaldin, N. A.; Rabe, K. M.; Wuttig, M.; Ramesh, R. *Science* **2003**, *299*, 1719–1722.
(7) Eerenstein, W.; Mathur, N. D.; Scott, J. F. *Nature* **2006**, *442*, 759–765.
(8) Catalan, G.; Scott, J. F. *Adv. Mater.* **2009**, *21*, 2463–2466.
(9) Martin, L. W.; Chu, Y. H.; Ramesh, R. *Mater. Sci. Eng., R* **2010**, *68*, 89–133.
(10) Singh, S. K.; Ishiwara, H.; Sato, K.; Maruyama, K. *J. Appl. Phys.* **2007**, *102*, 094109.
(11) Wu, J. G.; Wang, J. *J. Appl. Phys.* **2009**, *106*, 054115.
(12) Lee, C. C.; Wu, J. M. *Appl. Phys. Lett.* **2007**, *91*, 102906.
(13) Takahashi, K.; Tonouchi, M. *Jpn J. Appl. Phys., Part 2* **2006**, *45*, L755–L758.
(14) Qi, X.; Dho, J.; Tomov, R.; Blamire, M. G.; MacManus-Driscoll, J. L. *Appl. Phys. Lett.* **2005**, *86*, 062903.
(15) Ravindran, P.; Vidya, R.; Kjekshus, A.; Fjellvåg, H.; Eriksson, O. *Phys. Rev. B* **2006**, *74*, 224412.
(16) Li, J. F.; Wang, J. L.; Wuttig, M.; Ramesh, R.; Wang, N.; Ruette, B.; Pyatakov, A. P.; Zvezdin, A. K.; Viehland, D. *Appl. Phys. Lett.* **2004**, *84*, 5261–5263.
(17) Wu, J. G.; Wang, J. *Acta Mater.* **2010**, *58*, 1688–1697.
(18) Rana, D. S.; Takahashi, K.; Mavani, K. R.; Kawayama, I.; Murakami, H.; Tonouchi, M.; Yanagida, T.; Tanaka, H.; Kawai, T. *Phys. Rev. B* **2007**, *75*, 060405(R).
(19) Zhu, X. H.; Béa, H.; Bibes, M.; Fusil, S.; Bouzehouane, K.; Janque, E.; Barthélémy, A.; Lebeugle, D.; Viret, M.; Colson, D. *Appl. Phys. Lett.* **2008**, *93*, 082902.
(20) Lee, C. C.; Wu, J. M. *Appl. Phys. Lett.* **2007**, *91*, 102906.
(21) Wang, Y.; Lin, Y. H.; Nan, C. W. *J. Appl. Phys.* **2008**, *104*, 123912.
(22) Singh, S. K.; Ueno, R.; Funakubo, H.; Uchidai, H.; Kodai, S.; Ishiwara, H. *J. Appl. Phys.* **2005**, *44*, 8525–8527.
(23) Wu, J. G.; Kang, G. Q.; J. Liu, H.; Wang, J. *Appl. Phys. Lett.* **2009**, *94*, 172906.
(24) Wu, J. G.; Wang, J. *J. Appl. Phys.* **2010**, *107*, 034103.
(25) Wang, Y.; Wang, J. *J. Appl. Phys.* **2009**, *106*, 094106.
(26) Lu, S.; Xu, Z.; Zhai, J. *Thin Solid Films* **2010**, *518*, 5928.
(27) Kim, D. H.; Lee, H. N.; Biegalski, M. D.; Christen, H. M. *Appl. Phys. Lett.* **2008**, *92*, 012911.
(28) Ederer, C.; Spaldin, N. A. *Phys. Rev. Lett.* **2005**, *95*, 257601.
(29) Ravindran, P.; Vidya, R.; Kjekshus, A.; Fjellvåg, H.; Eriksson, O. *Phys. Rev. B* **2006**, *74*, 224412.
(30) Neaton, J. B.; Ederer, C.; Waghmare, U. V.; Spaldin, N. A.; Rabe, K. M. *Phys. Rev. B* **2005**, *71*, 014113.